

## Supporting Information

### **Distinct dual-isotopic signatures of major methane sources in South Asia**

Peng Yao<sup>1</sup>, Katja Belec<sup>1</sup>, Henry Holmstrand<sup>1</sup>, Josh Balacky<sup>1</sup>, Abdus Salam<sup>2</sup>, Krishnakant Budhavant<sup>3,4</sup>, Mohanan Remani Manoj<sup>1</sup>, Khaled Shaifullah Joy<sup>2,5</sup>, Md. Alamin Hossain<sup>2</sup>, Atinderpal Singh<sup>6</sup>, Anil Patel<sup>7,8,9</sup>, Neeraj Rastogi<sup>7</sup>, Chinmay Mallik<sup>10</sup>, Kirpa Ram<sup>11</sup>, Gyanesh Kumar Singh<sup>12,13</sup>, Örjan Gustafsson\*<sup>1</sup>

<sup>1</sup>Department of Environmental Science (ACES) and the Bolin Centre for Climate Research, Stockholm University, Stockholm 10691, Sweden

<sup>2</sup>Department of Chemistry, University of Dhaka, Dhaka 1000, Bangladesh

<sup>3</sup>Maldives Climate Observatory-Hanimaadhoo (MCOH), Maldives Meteorological Services, H. Dh. Hanimaadhoo 02020, Maldives

<sup>4</sup>Divecha Centre for Climate Change, Indian Institute of Science, Bangalore 560012, India

<sup>5</sup>Department of Chemistry, Drexel University, Philadelphia, PA-19104, United States

<sup>6</sup>Department of Environmental Studies, University of Delhi, Delhi, 110007, India

<sup>7</sup>Geosciences Division, Physical Research Laboratory, Ahmedabad 380009, India

<sup>8</sup>Bagchi School of Public Health, Ahmedabad University, Ahmedabad 380009, Gujarat, India

<sup>9</sup>The Climate Institute, Ahmedabad University, Ahmedabad 380009, Gujarat, India

<sup>10</sup>Department of Atmospheric Science, Central University of Rajasthan, Ajmer 305801, India

<sup>11</sup>Department of Chemistry, Institute of Science, Banaras Hindu University, Varanasi 221005, India

<sup>12</sup>Department of Civil Engineering, Indian Institute of Technology Kanpur, Kanpur, 208016, India

<sup>13</sup>Air Quality and Aerosol Metrology (AQAM) Group, National Physical Laboratory (NPL), Teddington, London TW11 0LW, UK

Corresponding: Örjan Gustafsson ([Orjan.Gustafsson@aces.su.se](mailto:Orjan.Gustafsson@aces.su.se))

## **Table of contents**

Sections S1–S3

Figs. S1–S5

Data S1–S2

## **S1. Isotopic source analysis of CH<sub>4</sub> from major sources in South Asia**

Isotopic source analysis of CH<sub>4</sub> from major sources in South Asia performed using the Keeling graphical approach based on the data obtained on source-specific samples collected in South Asia. Specific data available in Data S1.

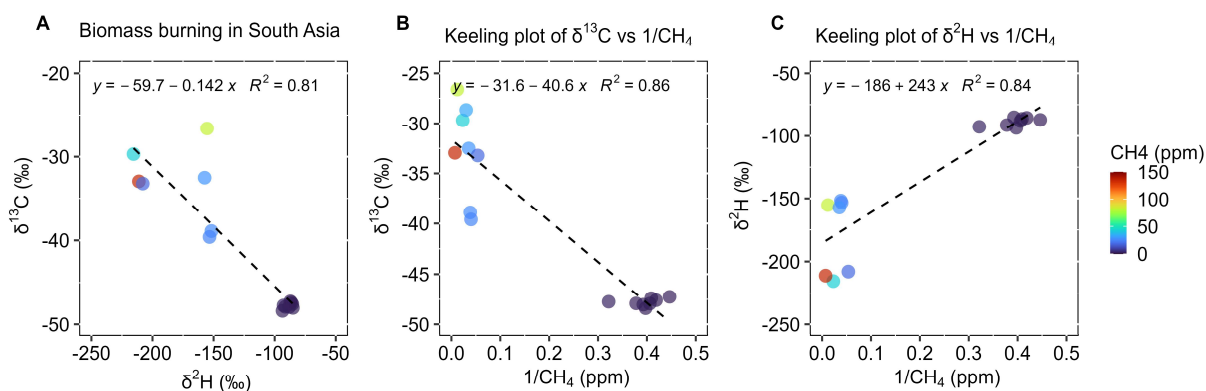


**Fig. S1. Mixing ratios and isotopic characteristics of CH<sub>4</sub> from biomass burning in South Asia. (A)** Synchronous variations in  $\delta^{13}\text{C}$  and  $\delta^2\text{H}$  of CH<sub>4</sub>. **(B)** Keeling plot for  $\delta^{13}\text{C}$ . **(C)** Keeling plot for  $\delta^2\text{H}$ .

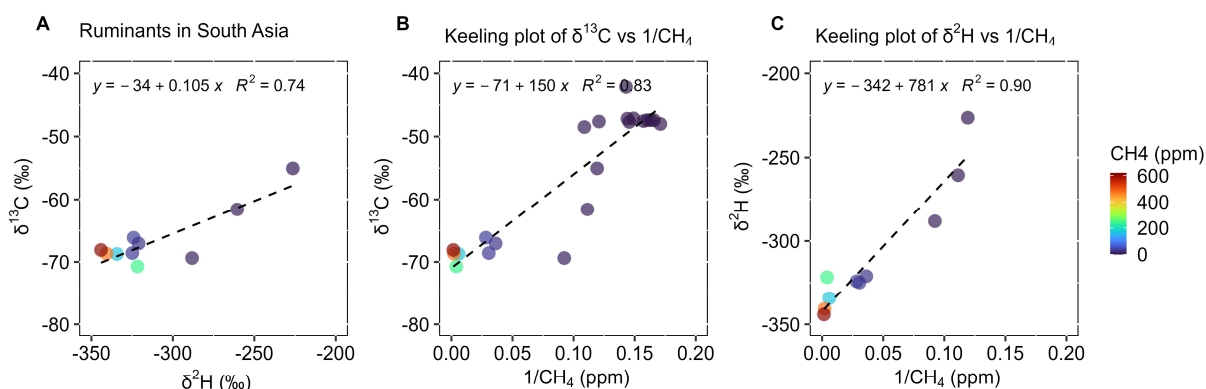


**Fig. S2. Mixing ratios and isotopic characteristics of CH<sub>4</sub> from ruminants in South Asia. (A)** Synchronous variations in  $\delta^{13}\text{C}$  and  $\delta^2\text{H}$  of CH<sub>4</sub>. **(B)** Keeling plot for  $\delta^{13}\text{C}$ . **(C)** Keeling plot for  $\delta^2\text{H}$ .

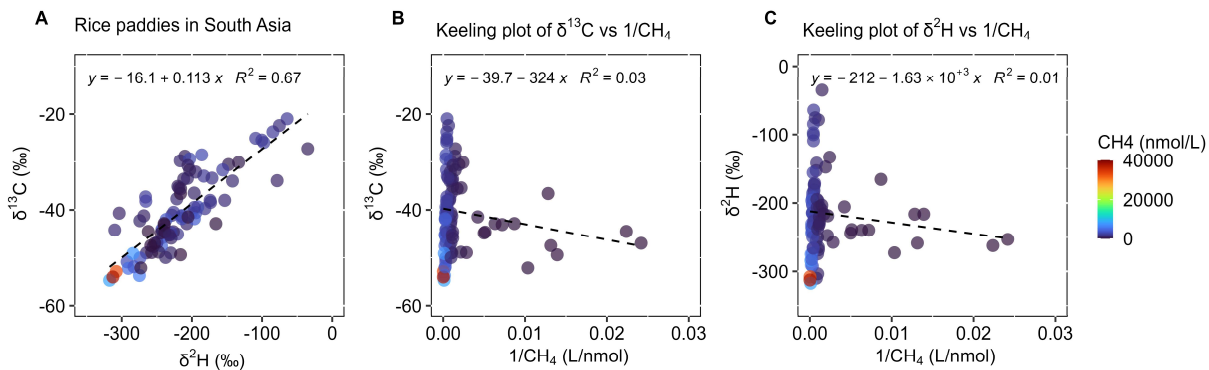


**Fig. S3. Mixing ratios and isotopic characteristics of CH<sub>4</sub> from rice paddies in South Asia.**

(A) Synchronous variations in  $\delta^{13}\text{C}$  and  $\delta^2\text{H}$  of CH<sub>4</sub>. (B) Keeling plot for  $\delta^{13}\text{C}$ . (C) Keeling plot for  $\delta^2\text{H}$ .

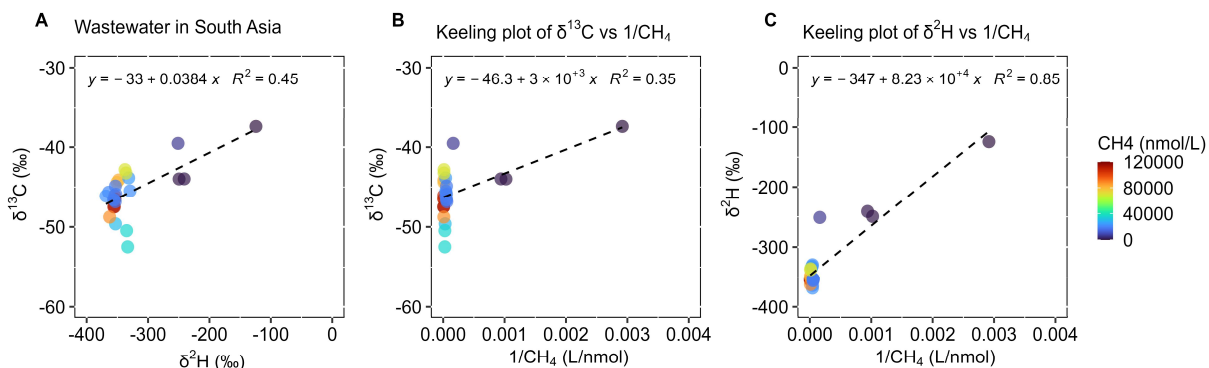


**Fig. S4. Mixing ratios and isotopic characteristics of CH<sub>4</sub> from wastewater in South Asia. (A)**

Synchronous variations in  $\delta^{13}\text{C}$  and  $\delta^2\text{H}$  of CH<sub>4</sub>. (B) Keeling plot for  $\delta^{13}\text{C}$ . (C) Keeling plot for  $\delta^2\text{H}$ .

## S2. Sample and background variations in Keeling and Miller-Tans methods

The application of the Keeling and Miller-Tans methods involves an inherent background-related issue. Here, we address this from first principles and systematically analyze different scenarios.

(1) The CH<sub>4</sub> concentrations in our source samples are very high, and therefore largely insensitive to background influence. Both Keeling and Miller-Tans approaches are fundamentally based on isotopic mass balance:

$$\delta_{obs} = \frac{c_{bg} \times \delta_{bg} + c_{source} \times \delta_{source}}{c_{bg} + c_{source}} \quad (S1)$$

When the source concentration is much higher than the background:

$$c_{source} \gg c_{bg} \quad (S2)$$

Eq. (S1) simplifies to:

$$\delta_{obs} \approx \delta_{source} \quad (S3)$$

This implies that when source concentrations are sufficiently high, the observed isotopic composition approaches that of the source. Therefore, high-concentration data points alone can provide a good approximation of the source isotopic signature, even without applying Keeling or Miller-Tans analyses.

(2) Why stable background conditions are often emphasized in Keeling and Miller-Tans analysis?

In practice, background conditions are never strictly constant, raising the question of how much variability is acceptable. Our answer is that it depends on the relative magnitude of source and background signals. To clarify this, we briefly revisit the mathematical structure of the Keeling approach.

In the Keeling formulation, background terms are embedded in the slope:

$$\delta_{obs} = c_{bg} \times (\delta_{bg} - \delta_{source}) \times \frac{1}{c_{obs}} + \delta_{source} \quad (S4)$$

As a result, variability in background leads to variations in the slope, which can distort the linear relationship (e.g., rotation or fan-shaped distributions in the data).

In contrast, the Miller-Tans formulation places the background contribution in the intercept:

$$\delta_{obs} \cdot c_{obs} = \delta_{source} \times c_{obs} + c_{bg} \cdot (\delta_{bg} - \delta_{source}) \quad (S5)$$

This means that the slope (i.e., the isotopic source signature) is less directly affected by background variability, while background fluctuations primarily influence the intercept, potentially increasing scatter without fundamentally altering the slope.

Nevertheless, both approaches reflect the combined influence of source and background variability. The key point is that the relative importance of background depends on the magnitude of source-driven variability. When source signals (variation of  $c_{source}$ ) are much stronger than background signal (variations of  $c_{bg}$ ), the derived Keeling intercepts and Miller-Tans slopes remain dominated by the source signal ( $c_{obs}$  variation dominated by  $c_{source}$ ), even if background variability is present. This is consistent with the case of  $c_{source} \gg c_{bg}$  (Eq. S2).

Conversely, when source-induced variations are comparable to background variability, even small background fluctuations may bias the inferred source signature. This situation may occur when source signals are weak or when observations are far away from the source but close to background conditions. For example, in some atmospheric observations over rice paddies,  $CH_4$  concentrations are close to background levels, such that background variability, although small in absolute terms, can still influence Keeling-derived source signatures.

(3) In our dataset, atmospheric background conditions are represented in the Keeling plots shown in the Supporting Information Figs. S1–S2, where low-concentration data points (around ~2 ppm) are included for ruminant and biomass burning samples, although their influence is negligible due to the dominance of high-concentration samples ( $c_{\text{source}} \gg c_{\text{bg}}$ ). For aqueous samples (rice paddies and wastewater), background methane is expected to be very low (effectively negligible), and the observed concentrations span several orders of magnitude, further confirming the dominance of source signals over background variability.



### **S3. Keeling and Miller-Tans methods in multi-source systems**

#### **S3.1 Interpretation boundaries of Keeling plots in multi-source systems**

The Keeling and Miller-Tans approaches are fundamentally formulated for systems in which a single source perturbs a relatively constant background. However, in natural environments, multiple sources often coexist. A common assumption is that both methods would reflect the isotopic signature of the mixed sources. Our analysis shows that this is generally not the case. Instead, both Keeling and Miller-Tans approaches tend to be biased toward the highest-concentration source, and contributions from weaker sources may be suppressed or even negligible when concentration differences are substantial.

Taking the Keeling plot as an example, this bias arises from the structure of the linear regression: high-concentration data points cluster near the origin in the x–y space and therefore exert a strong influence on the fitted line, whereas background points lie at the opposite end. Intermediate-concentration data points, located between these extremes, contribute comparatively little to the regression, resulting in a solution dominated by the highest-concentration source.

To illustrate this behavior, we performed Monte Carlo simulations of multi-source mixing. The baseline configuration includes a background with a concentration of  $2 \pm 0.002$  ppm and isotopic signatures of  $\delta^{13}\text{C} = -47.4\text{‰}$ , a microbial source ( $-65\text{‰}$ ), and a biomass burning source ( $-25\text{‰}$ ). Mixing was simulated under synchronous mixing conditions. We systematically varied the relative strengths of the microbial source, the biomass burning source, and the variability of the background.

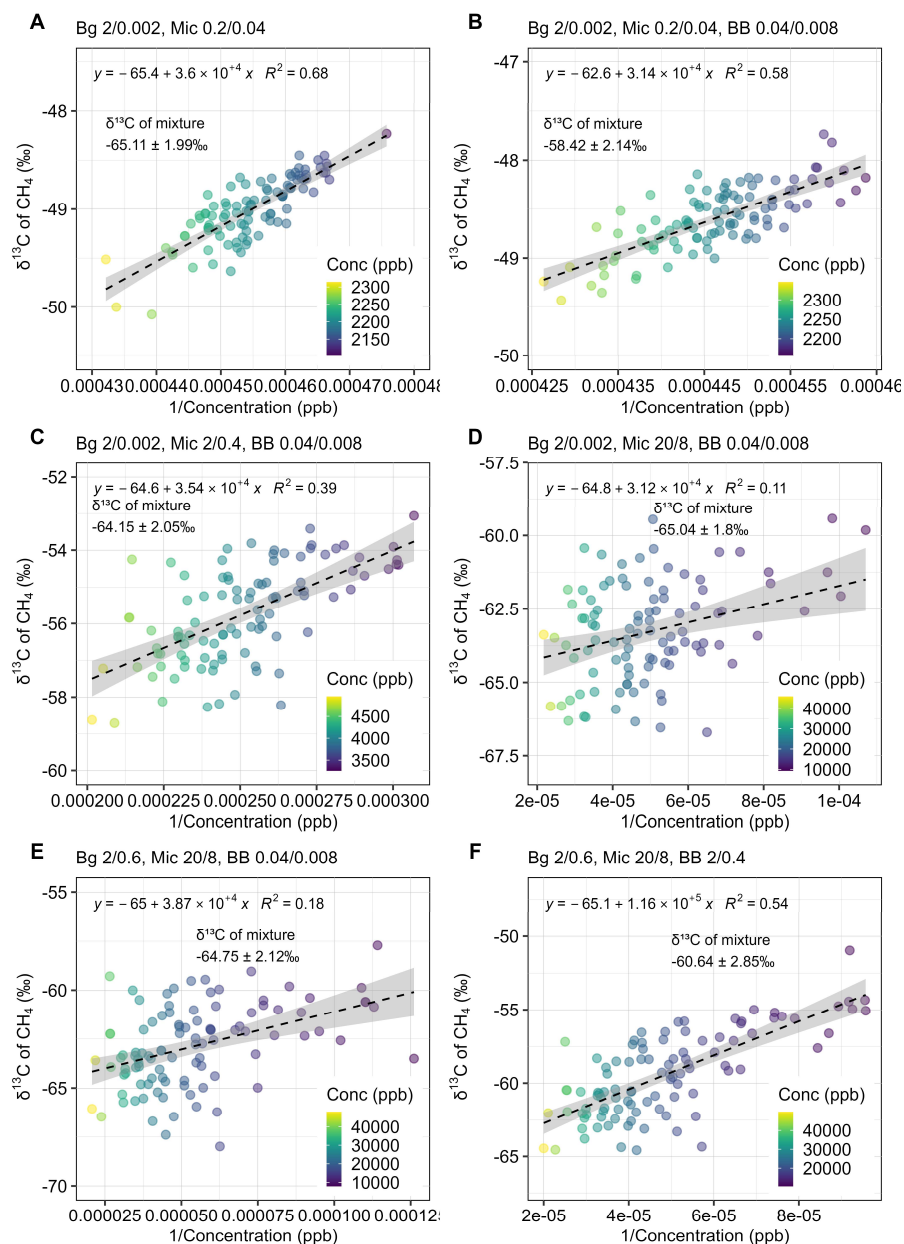


**Fig. S5. Interpretation boundaries of Keeling plots in multi-source systems.** Monte Carlo simulations are based on synchronous mixing of multi-source systems. **(A)** Background  $2 \pm 0.002$  ppm, microbial  $0.2 \pm 0.04$  ppm; **(B)** Background  $2 \pm 0.002$  ppm, microbial  $0.2 \pm 0.04$  ppm, biomass burning  $0.04 \pm 0.008$  ppm; **(C)** Background  $2 \pm 0.002$  ppm, microbial  $2 \pm 0.4$  ppm, biomass burning  $0.04 \pm 0.008$  ppm; **(D)** Background  $2 \pm 0.002$  ppm, microbial  $20 \pm 8$  ppm, biomass burning

$0.04 \pm 0.008$  ppm; **(E)** Background  $2 \pm 0.6$  ppm, microbial  $20 \pm 8$  ppm, biomass burning  $0.04 \pm 0.008$  ppm; **(F)** Background  $2 \pm 0.6$  ppm, microbial  $20 \pm 8$  ppm, biomass burning  $2 \pm 0.4$  ppm.

The simulation results (Fig. S5) consistently show that the Keeling method preferentially reflects the highest-concentration source. In Fig. S5A–S5B, the addition of a relatively small biomass burning source results in a mixed isotopic value of  $-58.4\text{‰}$ , whereas the Keeling-derived value ( $-62.6\text{‰}$ ) is clearly biased toward the higher-concentration microbial source ( $-65\text{‰}$ ). Similarly, comparison between Fig. S5A and Fig. S5C–S5D demonstrates that when the microbial source is sufficiently strong, weaker sources become negligible in the Keeling solution.

The influence of background variability was also examined. As shown by the comparison between Fig. S5D and Fig. S5E, background variability was increased from  $2 \pm 0.002$  ppm to  $2 \pm 0.6$  ppm, representing substantial fluctuations. However, the microbial source ( $20 \pm 8$  ppm) remained an order of magnitude higher than the background. Even under these conditions, background variability had little effect on the Keeling-derived source signature ( $-65\text{‰}$ ). In Fig. S5F, an additional biomass burning source ( $2 \pm 0.4$  ppm) was introduced, while the microbial source remained dominant ( $20 \pm 8$  ppm). Although the mixed isotopic value is  $-60.6\text{‰}$ , the Keeling-derived value ( $-65.1\text{‰}$ ) again closely reflects the highest-concentration microbial source.

These results demonstrate that, in multi-source systems, the Keeling approach tends to converge toward the isotopic signature of the dominant (highest-concentration) source, rather than the concentration-weighted mixture of all sources. This behavior contrasts with the common assumption that these methods directly reflect mixed-source signatures.

Furthermore, Fig. S5E–S5F show that when source concentrations exceed background levels by at least one order of magnitude, background variability becomes negligible, even under substantial fluctuations. This is consistent with Section S2.

### **S3.2 Reduced linearity of Keeling plots for rice paddies samples**

The reduced linearity observed in the Keeling plots for rice paddy samples can be attributed to the complex processes governing methane production and consumption in these systems. In flooded rice paddies, methane is primarily produced via microbial methanogenesis but may undergo partial oxidation during upward transport through the water column. Multiple production pathways generate methane with distinct initial isotopic compositions and concentrations, while oxidation processes progressively enrich the residual methane in heavy isotopes and reduce its concentration. Together, these processes create a continuum of methane with varying concentrations and isotopic signatures, rather than a single well-defined source.

As a result, the system cannot be fully captured by a simple two-component mixing framework (source + background). Instead, multiple sources and partially oxidized methane coexist. Although some samples exhibit concentrations orders of magnitude above the background set by atmospheric methane dissolved in water ( $c_{\text{source}} \gg c_{\text{bg}}$ ), the combination of multiple sources and partial oxidation introduces additional variability.

In the Keeling formulation, background contributions are incorporated into the slope. Under multi-component conditions, weaker sources and partially oxidized methane effectively behave as variable background contributions, leading to deviations from linearity and reduced robustness of the regression. In contrast, the Miller-Tans formulation incorporates background contributions into

the intercept. When concentrations span several orders of magnitude, the slope is primarily controlled by the dominant, highest-concentration endmember (i.e., the least oxidized methane), resulting in a more stable and interpretable linear relationship.

Therefore, while both approaches tend to reflect the isotopic signature of the highest-concentration source, the Miller-Tans method is less sensitive to the presence of background variability, multiple weak sources, and partial oxidation. It is thus better suited for systems such as rice paddies, where methane arises from multiple sources and undergoes significant in situ oxidation.

### **S3.3 Atmospheric observations of rice paddy methane**

Most previous studies of methane isotopic signatures from rice paddies have relied on atmospheric sampling above the fields, combined with Keeling or Miller-Tans analyses to infer source signatures. The validity of atmospheric measurements for characterizing rice paddy methane depends on several fundamental factors.

First, as discussed in Section S3.1, in multi-source systems, both Keeling and Miller-Tans approaches tend to converge toward the dominant (highest-concentration) source. In rice paddy environments, where multiple source and partial oxidation may coexist, the inferred isotopic signature may therefore primarily reflect the highest-concentration source, while weaker sources are effectively masked.

Second, atmospheric measurements may be influenced by surrounding emission sources, such as ruminants, biomass burning, or domestic waste. This interference becomes particularly important when rice paddy emissions are not sufficiently strong to dominate the local isotopic signal.

Third, methane emitted from rice paddies may originate from multiple pathways and undergo in situ processing. For example, plant-mediated transport can transfer methane from subsurface layers to the atmosphere, potentially including both relatively unoxidized methane and methane that has been partially oxidized during transport through the water column. When these components are mixed in the atmosphere, Keeling and Miller-Tans analyses will again tend to reflect the dominant emission component, while other components may be underrepresented.

Finally, when rice paddy emissions are weak, the resulting atmospheric perturbation may be small and close to ambient methane levels. In such cases, source-induced variability becomes comparable to background variability, violating the assumptions underlying both Keeling and Miller-Tans methods. Consequently, the inferred source signatures may be strongly influenced by background fluctuations, which may explain why some studies report values close to atmospheric methane.

Overall, these considerations highlight that atmospheric sampling over rice paddies may be subject to uncertainties, depending on the relative strength of emissions, the presence of surrounding sources, and the complexity of methane production and oxidation processes. In this context, water-phase sampling provides a complementary approach to better constrain source signatures and to evaluate the representativeness of atmospheric observations.

### **S3.4 Aquatic observations of methane in rice paddies**

In this study, we analyzed dissolved methane in paddy water, providing an alternative perspective to assess the representativeness of isotopic signatures derived from atmospheric measurements. Aquatic observations of methane in rice paddies are also subject to complexities, among which

methane oxidation within the water column is a key factor. As discussed in Section S2, when methane concentrations are sufficiently high ( $c_{\text{source}} \gg c_{\text{bg}}$ ), the observed isotopic composition approximates the source value ( $\delta_{\text{obs}} \approx \delta_{\text{source}}$ ). Our observations indicate that even high-concentration samples can exhibit multiple isotopic values, reflecting the coexistence of multiple methane sources.

The complexities arise from the coupled effects of methane production, oxidation, and transport processes. For example, plant-mediated transport can transfer both relatively unoxidized and partially oxidized methane from subsurface layers to the atmosphere. In addition, mixing and diffusion within the water column redistribute methane, leading to spatial and temporal heterogeneity in both concentration and isotopic composition. As a result, water-phase measurements provide access to a wider range of methane states and processes than atmospheric observations.

Our water-based sampling approach therefore provides a complementary perspective for constraining methane isotopic source signatures. First, high-concentration methane measured in water samples directly constrains the isotopic composition of the dominant source. Under conditions where  $c_{\text{source}} \gg c_{\text{bg}}$ , even without applying Keeling or Miller-Tans analyses, high-concentration samples already approximate the source signature. These high-concentration points, even if partially oxidized, retain largely consistent isotopic values. Using multiple analytical methods, we derive representative isotopic values, and the Miller-Tans method effectively captures the highest-concentration, minimally oxidized source.

Second, to account for the complexity of methane production and transport, we report concentration-weighted isotopic values. These values integrate contributions from multiple

sources and methane at different stages of oxidation and transport, including both unoxidized and partially oxidized components, as well as spatial heterogeneity within the water column.

Finally, the isotopic source signatures adopted in this study are derived from Miller-Tans analyses applied to water-phase data. While conceptually consistent with atmospheric approaches, water sampling benefits from conditions where source signals are dominant and better constrained, reducing uncertainties associated with background variability and external source interference, which can be an interference in atmospheric measurements.